

Direct probes of R -parity-violating supersymmetric couplings via single-top-squark production

Edmond L. Berger, B. W. Harris, and Z. Sullivan

High Energy Physics Division, Argonne National Laboratory, Argonne, Illinois 60439

(December 14, 2000)

Abstract

We study the s -channel production of a *single* top squark in hadron collisions through an R -parity-violating mechanism, examining in detail the case in which the squark decays through an R -parity-conserving process into a bottom quark, a lepton, and missing energy. We show that the top squark can be discovered if its mass is less than 400 GeV, or that the current bound on the size of the R -parity-violating couplings can be reduced by up to one order of magnitude with existing data and by two orders of magnitude at the forthcoming run II of the Fermilab Tevatron.

PACS numbers: 11.30.Pb, 12.60.Jv, 14.80.Ly

Typeset using REVTeX

I. INTRODUCTION

In supersymmetric extensions of the standard model, particles may be assigned a new quantum number called R -parity (R_p) [1]. The particles of the standard model are R_p even, and their corresponding superpartners are R_p odd. If R_p is conserved, as is often assumed, superpartners must be produced in pairs, each of which decays to a final state that includes at least one stable lightest supersymmetric particle (LSP). If R_p is not conserved, then many of the experimental signatures of supersymmetry that are usually studied may not be observable. Hence, it is important to determine whether R_p -violation occurs and, if so, whether the effects are significant in collider experiments. Current bounds on possible R_p -violating couplings are relatively restrictive for the first generation of quarks and leptons but are much less so for states of the second and third generations [2].

Searches for R_p violation often focus on the decays of superpartners under the assumption that they are produced in pairs via an R_p -conserving interaction [2]. However, squarks and gluinos are generally predicted to be relatively heavy, and therefore their pair-production cross sections incur large phase space suppressions at Fermilab Tevatron energies.

In this paper, we expand and improve upon our previous proposal [3] to probe R_p -violating couplings by searching for the s -channel production of a *single* squark through an R_p -violating mechanism [4]. The greater phase space afforded by the production of one heavy particle, instead of two, will allow searches to reach much higher masses than those based on traditional squark pair-production. Further, since the R -parity violation occurs in production, the cross section will provide a direct measure of the individual R_p -violating couplings.

In Sec. II, we describe the baryon-number-violating portion of the R_p -violating Lagrangian and establish our notation and conventions. The cross section for pair-production of top squarks is small compared to that for the process $qq' \rightarrow \tilde{t}_1$ that can proceed through R_p -violating couplings. The R_p -violating couplings are weakly constrained by quantum corrections to particle decays and neutral meson mixing. In order to capitalize on the enhanced

rate for single production it is necessary to examine the decay products of the top squarks. We address in Sec. III the possibility that decay will occur through an R_p -violating process into two hadronic jets and show that this rate is far below that for standard quantum chromodynamics (QCD) production of jet pairs.

In Sec. IV, we study observability of single top squarks by focusing on the clean R_p -conserving decay, $\tilde{t}_1 \rightarrow b\tilde{\chi}_1^+$, with $\tilde{\chi}_1^+ \rightarrow l^+ + \nu_l + \tilde{\chi}_1^0$. Here, l is an electron or muon, and the $\tilde{\chi}_1^+$ and $\tilde{\chi}_1^0$ are the chargino and lowest-mass neutralino states of the minimal supersymmetric standard model (MSSM) [5]. We introduce a method to extract a top-squark mass peak from the standard model background, principally W + hadronic jets. To study the effects of parton showering, hadronization, and color-recombination, we simulate the signal with the HERWIG [6] Monte Carlo event generation program. The response of a typical experimental detector is modeled using the full SHW detector simulation package [7]. We explore a wide range of the parameter space of the minimal supergravity (mSUGRA) model of supersymmetry breaking [8]. Each of these improvements renders the analysis more realistic and strengthens the conclusions reached in our earlier work [3].

Our conclusions are stated in Sec. V. For top squarks with mass $m_{\tilde{t}_1} < 400$ GeV, we show that discovery at the level of five standard deviations (5σ) is possible at $\sqrt{S} = 2$ TeV with an integrated luminosity of 2 fb^{-1} , provided that the R_p -violating couplings $\lambda'' > 0.02 - 0.1$. Otherwise, a 95% confidence-level exclusion limit can be set for λ'' as a function of the mass up to about 500 GeV. For the lower integrated luminosity and energy of the existing run I data, values of $\lambda'' > 0.05 - 0.2$ can be excluded at the 95% confidence level if $m_{\tilde{t}_1} = 165 - 350$ GeV. These limits would constitute a significant improvement over the current 95% confidence-level upper bounds of $\lambda'' \lesssim 1$ for squarks of the third generation [2]. With the large increase in cross section at the CERN Large Hadron Collider (LHC), the discovery region and limits may be improved by another order of magnitude in λ'' and to top-squark masses approaching 1 TeV. The discovery reach, or exclusion limits, at the Tevatron and LHC depend almost exclusively on the value of the top-squark mass, largely independent of other supersymmetric parameters.

A lower limit of about 165 GeV on the accessible value of the top squark mass via our method is determined by the selections made on the b jet and lepton momenta in order to achieve a satisfactory signal to background ratio. An upper bound of about 550 GeV is set by the event rate. To explore values of the top-squark mass well below that of the top quark, it appears necessary to combine results of our analysis with those based on pair production of top squarks.

For the values of the R -parity-violating couplings of interest to us, the R -parity-violating width of the $\tilde{\chi}_1^0$ remains negligible and for all practical purposes the $\tilde{\chi}_1^0$ LSP is stable. We leave to future work the exploration of larger values of R -parity-violating couplings and consequent decays of the $\tilde{\chi}_1^0$ within the fiducial region of detectors.

II. MSSM SUPERPOTENTIAL AND NOTATION

In general it is possible to have R_p -violating contributions to the MSSM superpotential that violate baryon- or lepton-number. However, limits on the proton decay rate severely restrict their simultaneous presence. In this paper, we assume the existence of only a baryon-number-violating coupling of the form [9],

$$\mathcal{W}_{R_p} = \lambda''_{ijk} U_i^c D_j^c D_k^c . \quad (1)$$

Here, U_i^c and D_i^c are right-handed-quark singlet chiral superfields, i, j, k are generation indices, and c denotes charge conjugation. This form of the superpotential fixes our choice of normalization of λ''_{ijk} . It is equal to $\lambda''_H/2$, where λ''_H is the coupling used in HERWIG [6].

In four-component Dirac notation, the Lagrangian that follows from this superpotential term is

$$\begin{aligned} \mathcal{L}_{\lambda''} = & -2\epsilon^{\alpha\beta\gamma} \lambda''_{ijk} \left[\tilde{u}_{Ri\alpha} \overline{d_{j\beta}^c} P_R d_{k\gamma} + \tilde{d}_{Rj\beta} \overline{u_{i\alpha}^c} P_R d_{k\gamma} \right. \\ & \left. + \tilde{d}_{Rk\gamma} \overline{u_{i\alpha}^c} P_R d_{j\beta} \right] + h.c. , \end{aligned} \quad (2)$$

where $j < k$.

For production of a right-handed top squark via an s -channel subprocess $\bar{d}_j \bar{d}_k \rightarrow \tilde{t}_R$ the relevant couplings are λ''_{312} , λ''_{313} , and λ''_{323} . The most direct limits on these couplings come from the measurement of R_l , the partial decay width of the Z boson to hadrons over its partial decay width to leptons. The analysis of R_l provides 95% confidence-level upper bounds of $\lambda''_{3jk} \lesssim 1$ [2]. The limits, given as a function of mass in the third paper of Ref. [2], are approximately $\lambda''_{312} < 1.52 + 0.425 \times (m_{\tilde{t}_1}/100 \text{ GeV})$, and $\lambda''_{313,323} < 0.585 + 0.162 \times (m_{\tilde{t}_1}/100 \text{ GeV})$.

Subsequent to our Letter [3], it was argued that rare B^+ decays and $K^0-\bar{K}^0$ mixing constrain λ''_{3jk} strongly [10]. The analysis of these decays *indirectly* constrains *products* of different λ''_{3jk} , whereas the method we propose may be used to *directly probe each coupling independently*.

Shown in Fig. 1 is the Feynman diagram for s -channel production of a single top squark via the partonic subprocess $d + s \rightarrow \tilde{t}_R$. The right-handed top-squark interaction state is related to the mass eigenstates by $\tilde{t}_R = -\tilde{t}_1 \sin \theta_{\tilde{t}} + \tilde{t}_2 \cos \theta_{\tilde{t}}$. For simplicity of notation, and motivated by models where $\sin \theta_{\tilde{t}} \approx 1$, we present results in terms of a measurement of \tilde{t}_1 . In general, the results are valid for whichever mass eigenstates contain some amount of the right-handed top squark.

The color- and spin-averaged cross section for inclusive \tilde{t}_1 production is

$$\sigma = \frac{2\pi}{3S} \sin^2 \theta_{\tilde{t}} \sum_{j < k} |\lambda''_{3jk}|^2 \Phi_{jk}(\tau), \quad (3)$$

where S is the square of the hadronic center of mass energy, and $\tau = m_{\tilde{t}_1}^2/S$. The integrated parton luminosity Φ_{jk} contains a convolution of the parton distribution functions (PDF's): $d \otimes s$, $d \otimes b$, and $s \otimes b$, where d , s , and b label the PDF's of the down, strange, and bottom quarks, respectively. The cross section for \tilde{t}_2 production is the same as above but with $\sin^2 \theta_{\tilde{t}}$ replaced by $\cos^2 \theta_{\tilde{t}}$.

The mass dependences of the next-to-leading order (NLO) cross sections for R_p -violating single production [11] and R_p -conserving pair production [12] of top squarks differ significantly, as shown in Fig. 2. Results are presented for the sum of \tilde{t}_1 and $\tilde{\bar{t}}_1$ production and

couplings $\lambda''_{3jk} = 0.1$. Even if λ''_{3jk} is reduced to 0.01, two orders of magnitude below the current bound, the single-top-squark rate exceeds the pair rate for $m_{\tilde{t}_1} > 100$ GeV. The parton luminosities determine that the contribution to the total cross section of the terms proportional to $\lambda''_{312} : \lambda''_{313} : \lambda''_{323}$ is about $0.72 : 0.24 : 0.04$ at $m_{\tilde{t}_1} = 200$ GeV.

In order to simplify the explanation of some of the general features of this study, we define $\lambda'' \equiv \lambda''_{312} = \lambda''_{313} = \lambda''_{323}$. The results for independent couplings are related by a simple functional form and are presented below. Since the cross section in Eq. (3) is proportional to the square of the product $\lambda''_{3jk} \sin \theta_{\tilde{t}}$, the limits on λ''_{3jk} discussed and derived here for \tilde{t}_1 are really limits on this product. Correspondingly, the limits for \tilde{t}_2 are really on $\lambda''_{3jk} \cos \theta_{\tilde{t}}$.

III. R -PARITY-VIOLATING DECAYS

In the R_p -violating MSSM, the right-handed up-type squark \tilde{u}_R can decay into quark pairs $\tilde{u}_R \rightarrow \bar{d}_j + \bar{d}_k$ via the λ'' couplings. The decay width of the top-squark mass eigenstate into two jets is

$$\Gamma(\tilde{t}_1 \rightarrow jj) = \frac{m_{\tilde{t}}}{2\pi} \sin^2 \theta_{\tilde{t}} \sum_{j < k} |\lambda''_{3jk}|^2. \quad (4)$$

If $\lambda'' \gtrsim 2$, the width of the top squark is greater than its mass. This is true generally for *any* squark and *any* baryon-number-violating coupling. Hence, there is a practical upper limit on λ'' for the model to contain narrow resonances.

In Fig. 3, we present the dijet mass distribution that results from the R_p -violating decays of singly-produced top squarks with $\lambda'' = 1$. We simulate the signal for various masses with a matrix-element calculation that uses HELAS [13] subroutines. For comparison, we also reproduce the data published by the CDF collaboration [14]. We apply the same cuts in our simulation as in the data. The signal to background ratio (S/B) in the dijet channel is less than $(\lambda'')^2/100$ for any mass. Because of the overwhelming jet rate from standard strong interaction processes, we confirm the expectation [4] that the dijet data can neither exclude R -parity-violating production and decay of top squarks nor provide useful bounds on λ'' .

IV. R -PARITY-CONSERVING DECAYS

In this section we focus on probes of λ'' couplings through R_p -conserving decay modes of the top squark. If kinematically allowed, a heavy top squark decays into a bottom quark (b) and the lightest chargino $\tilde{\chi}_1^+$. If $m_{\tilde{t}_1} < m_{\tilde{\chi}_1^+} + m_b$, the decay would occur into a charm quark and a neutralino via flavor changing loop diagrams [15]. For the top squark masses of interest to us, and in the context of the mSUGRA model in which we work, the decay $\tilde{t}_1 \rightarrow b + \tilde{\chi}_1^+$ dominates. Other channels open at large \tilde{t}_1 masses (e.g. decay into a top quark and the lightest neutralino, $t + \tilde{\chi}_1^0$), but their decay widths are less than half of the R_p -conserving decay width for the masses we consider. The chargino typically undergoes a three-body decay into a neutralino and the decay products of a W boson. Since it is challenging to observe an all-jets plus missing energy mode, we concentrate on the case where the final state is a bottom quark plus a neutralino and an electron or muon from the chargino decay.

We show the branching fractions of the top squark into two jets and of the cascade ($\tilde{t}_1 \rightarrow b\tilde{\chi}_1^+ \rightarrow bl^+\nu_l\tilde{\chi}_1^0$) as a function of λ'' in Fig. 4. The R_p -violating branching fraction of the chargino is also shown. The R_p -conserving decay dominates for small λ'' . For both the top squark and the chargino, the width into jets increases when λ'' is large. The branching fraction into the signal mode is inversely proportional to $(\lambda'')^2$. However, in seen in Eq. (3), the production cross section is proportional to $(\lambda'')^2$, and thus the entire cross section behaves as

$$\begin{aligned} \sigma(p\bar{p} \rightarrow bl^+\nu_l\tilde{\chi}_1^0) &= \sigma(p\bar{p} \rightarrow \tilde{t}_1) \times \text{BR}(\tilde{t}_1 \rightarrow b\tilde{\chi}_1^+) \\ &\quad \times \text{BR}(\tilde{\chi}_1^+ \rightarrow l^+\nu_l\tilde{\chi}_1^0) \\ &\sim \lambda''^2 \frac{1}{\lambda''^2 + a\Gamma_{\tilde{t}_1}^{R_p}} \frac{1}{\lambda''^2 + b\Gamma_{\tilde{\chi}_1^+}^{R_p}}. \end{aligned} \quad (5)$$

In Eq. (5), $\Gamma_{\tilde{t}_1}^{R_p}$ and $\Gamma_{\tilde{\chi}_1^+}^{R_p}$ are the R_p -conserving partial decay widths of the lightest top squark and chargino, respectively, and a and b are appropriate proportionality factors.

In the presence of R_p -violating couplings, the neutralino is not stable. There are three

decay scenarios that potentially give rise to distinct signatures in the detector. In the first scenario, only the λ''_{3jk} couplings are larger than 10^{-4} – 10^{-5} . In this case, the neutralino must decay through an off-shell top quark and off-shell top squark into a five-body final state. A neutralino whose mass is 100 GeV or less has decay lifetime $c\tau > 100/(\lambda'')^2$ m (see Fig. 26 of Ref. [2]) and decays far outside the detector. Hence, the signature of the neutralino is simply missing energy in the detector. In this paper we address the case where the neutralino either decays outside of the detector volume or leaves remnants that are too soft to identify. The signal is a tagged b -jet, an electron or muon, and large missing transverse energy. The main backgrounds are single-top-*quark* production, and W +jets processes that either contain a bottom quark or have a jet that is mis-tagged as a b -jet.

If other baryon-number-violating couplings are large, then the neutralino can decay inside the detector. The signature of this second scenario includes two or three extra jets that appear to come from the primary vertex. The modeling of the energy distributions of these jets depends on explicit choices of some parameters. In an interesting third possibility, at least one of the first- or second-generation couplings, $\lambda''_{123}, \lambda''_{2jk}$, is greater than 10^{-3} . The decay may either have a displaced vertex or occur in a calorimeter. These possibilities warrant further study.

A. Simulation

In order to include the effects of parton showering and hadronization, we simulate the signal with the Monte Carlo program HERWIG 6.1 [6], a version that includes R_p -violating interactions, and we use the SHW 2.3 [7] detector simulation package. The SHW package provides a reasonably close approximation of the expected acceptance of the upgraded CDF and D0 detectors to signal and background processes. It determines what charged tracks and calorimeter energies the detector would record and supplies information about the trigger and reconstructed states such as electrons, muons, and hadronic jets, including b - and c -jet tagging.

In addition to interfacing SHW to HERWIG, we make a few modifications for this study. We include the NLO K -factors calculated in Ref. [11]. A k_T cluster algorithm [16] for hadronic jets is added to provide an infrared-safe way of combining calorimeter towers. We use a k_T cone size of 1, similar to a fixed cone size of $\Delta R = 0.7$. We also correct for the typical out-of-cone and threshold energy losses in the jet reconstruction of about 4 GeV per jet. After this correction, we find that the radiation, showering, and color-reconnection modeled in HERWIG 6.1 have little effect on the distributions of the reconstructed objects with respect to the parton level results presented in Ref. [3].

We use impact-parameter tagging as defined in SHW to tag b -jets and to acquire the energy-dependent rate for charm quarks to fake bottom quarks. For a conservative estimate of the background, we choose the mis-tag rate for light-quark jets to be the greater of 0.5% or the output of SHW. The event trigger is either an electron or muon that passes the SHW triggering conditions, typically a transverse energy $E_{Tl} > 15$ GeV, as listed in Table I. The missing transverse energy E_T is calculated for the entire detector (calorimeters plus muon chambers).

In Table I, we provide the geometric acceptance of a detector as defined by SHW. The lepton-finding algorithm in SHW is based on the CDF run I geometry and thus covers a slightly smaller pseudorapidity region than used in our original Letter (see Table I of Ref. [3]). There is an additional loss of 20% of the leptons compared with our initial assumptions due to modeling of detector efficiencies. After these detector effects and the slightly different choice of cuts are accounted for, the full simulation is in complete agreement with the exact leading-order matrix element calculation used in our Letter [3]. We also confirm that adding Eq. (3) to PYTHIA 6.131 [17] produces the same results, an independent confirmation that color-recombination ambiguities, present for finite baryon-number-violating couplings [18], do not impact the results.

The backgrounds are modeled with tree-level matrix elements obtained from MADGRAPH [19] convolved with leading-order CTEQ5L [20] parton distribution functions, at a hard scattering scale $\mu^2 = \hat{s}$. In order of importance, these backgrounds arise from produc-

tion and decay of the standard model processes Wc , with a charm quark c that is mistaken for a b ; Wj , with a hadronic jet that mimics a b ; $Wb\bar{b}$; $Wc\bar{c}$; and single-top-*quark* production via Wg fusion. The tagging efficiencies and geometry are the same as used in SHW. In an experimental analysis, the Wj background would be normalized by the data. To simulate the resolution of the hadron calorimeter for background events, we smear the jet energies with a Gaussian whose width is $\Delta E_j/E_j = 0.80/\sqrt{E_j} \oplus 0.05$ (added in quadrature). To verify the accuracy of our background estimation, we perform a full HERWIG and SHW simulation for the Wj background. The relevant distributions match those of the matrix element calculation to better than 10%. As explained below, numerical limits on the couplings are insensitive to small uncertainties in the background.

The b quark recoils against the chargino in the primary decay of the top squark. Thus the measured E_T spectrum for the b -jet is peaked near the kinematic limit

$$E_{Tb}^{\max} = \frac{m_{t_1}^2 - m_{\tilde{\chi}_1^+}^2 + m_b^2}{2m_{t_1}}. \quad (6)$$

An estimate of the mass difference between the top squark and chargino may be obtained if a prominent peak is found in the E_{Tb} spectrum. If we invert this equation, a kinematic constraint appears on the lowest top-squark mass that may be probed with this method, $m_{t_1} > m_{\tilde{\chi}_1^+} + E_{Tb}^{\text{cut}}$.

In Fig. 5, we show the E_T spectrum for the b -jet, tagged by the SHW impact-parameter method, for two different top squark masses, as well as the $Wb\bar{b}$ background. The background falls rapidly as a function of E_{Tb} . The b -jet from the single-top-quark background peaks near 60 GeV, but it makes a small contribution after cuts. The cut on the E_T of the b -jet is chosen to ensure a reasonable tagging efficiency (greater than 50%). Variation of this number between 30 GeV and 80 GeV has no effect on the significance of the signal as long as the signal remains kinematically allowed.

The lepton from chargino decay ($\tilde{\chi}_1^+ \rightarrow l^+ \nu_l \tilde{\chi}_1^0$) tends to be soft since much of the energy goes into the mass of the neutralino, and the rest is split by the three-body decay. In contrast, the lepton in the background comes from decay of a real W . It clusters around 40

GeV (1/2 of the W mass) and has a broad rapidity distribution. After reconstruction, the remaining events are distributed from 20 GeV to 70 GeV (see Fig. 6). Given the different shapes of the p_T spectra, it is possible to impose a hard “lepton veto” of 45 GeV to reduce the background with very little effect on the signal. This cut is most useful for increasing the purity of the Tevatron run I sample.

The extra hard jets in the $Wb\bar{b}$, $Wc\bar{c}$, and single-top-quark backgrounds distinguish these processes from the signal. Since extra jets in the signal arise only in radiation from the hard process in 10 – 20% of the events, we consider a “jet veto” that removes any event containing a second jet with $E_{Tj} > 30$ GeV. The main effect of this cut is to improve the purity of the sample (S/B). The “jet veto” improves the significance (S/\sqrt{B}) by a few percent at the Tevatron for high $m_{\tilde{t}_1}$, but decreases it by a few percent at the LHC for all masses. This cut is most useful if evidence of the signal is found and a higher purity confirmation is desired.

B. Results

To obtain numerical results, we adopt a minimal supergravity framework [8] to compute the masses of the top squark and its decay products and the relevant branching fractions. Later, by varying the parameters of the model, we show that it is the top-squark mass itself that is the dominant variable in probing the λ'' couplings.

We begin with common scalar and fermion masses of $m_0 = 100$ GeV and $m_{1/2} = 150$ GeV, respectively, at the Grand Unified Theory (GUT) scale. We choose a trilinear coupling $A_0 = -300$ GeV and the ratio of the Higgs vacuum expectation values $\tan\beta = 4$. The absolute value of the Higgs mass parameter μ is fixed by electroweak symmetry breaking and is assumed positive. Superpartner masses and decay widths are calculated with ISAJET 7.50 [21] and ISAWIG 1.1 [6]. After evolution from the GUT scale to the weak scale, for this set of parameters one obtains $m_{\tilde{t}_1} = 167$ GeV, $m_{\tilde{\chi}_1^0} = 53$ GeV, $m_{\tilde{\chi}_1^\pm} = 95$ GeV, and $\sin\theta_{\tilde{t}} = 0.8$. In Fig. 7 we show the mass contours for the \tilde{t}_1 , the $\tilde{\chi}_1^0$, and the $\tilde{\chi}_1^\pm$. A recent experimental lower bound of 80.5 GeV on the mass of the lightest chargino $\tilde{\chi}_1^\pm$ [22] is used to

exclude regions (ex) of small $m_{1/2}$. Regions in which tachyonic particles would be generated, electroweak symmetry would not be broken, or in which the lightest supersymmetric particle (LSP) is not the lightest neutralino $\tilde{\chi}_1^0$ are marked as excluded theoretically (th).

The top-squark mass grows slowly with m_0 . The lightest chargino $\tilde{\chi}_1^+$ and neutralino $\tilde{\chi}_1^0$ masses are nearly independent of the common scalar mass m_0 . In order to focus principally on top-squark mass dependence, we vary m_0 and keep the other supersymmetric parameters fixed. Since the gaugino masses depend primarily on the choice of $m_{1/2}$, variation of m_0 allows us to vary $m_{\tilde{t}_1}$ without an appreciable change in the masses of the decay products and only a slow rise of $\sin \theta_{\tilde{t}}$ to 1. The results obtained in this section therefore depend primarily on the top-squark mass and on which decay channels are allowed kinematically.

We reconstruct a longitudinally invariant mass $M \equiv M_T + \cancel{p}_T$, where $M_T = \sqrt{m_X^2 + p_{TX}^2}$ is the transverse mass for the lepton $- b$ -jet system ($m_X^2 = P_X^2$, $P_X^\mu = P_b^\mu + P_l^\mu$), and \cancel{p}_T is the magnitude of the missing transverse momentum for the event. The mass M has the useful feature that it produces a peak at $m_{\tilde{t}_1} - m_{\tilde{\chi}_1^0} + m_b$. Reconstruction of the peak provides a measure of the mass difference between the top squark and the lightest neutralino. We replace the mass definition of Ref. [3] because it is not longitudinally boost-invariant and hence is more sensitive to the detailed modeling of the decays.

In Fig. 8 we show a representative reconstructed mass M distribution at run II of the Tevatron ($\sqrt{S} = 2$ TeV) for a top squark of mass $m_{\tilde{t}_1} = 255$ GeV. The coupling $\lambda'' = 0.1$ is chosen to be one order-of-magnitude below the current bound. The total background (B) is shown with its components: Wj includes Wc , Wj , $Wb\bar{b}$, and $Wc\bar{c}$; t includes all single-top-quark production modes. Both the “lepton veto” and “jet veto” are applied in this figure. The decrease in the background for $M < 140$ GeV evident in the figure is attributed to the cuts we impose.

It should be easy to observe the sizeable deviation from the background distribution associated with a top squark produced with coupling strength $\lambda'' = 0.1$, shown in Fig. 8. In Fig. 9 we show the distribution in M for the minimum value of $\lambda'' = 0.04$ required for a 5σ discovery with an integrated luminosity of 2 fb^{-1} at $\sqrt{S} = 2$ TeV. The significance is

calculated in a bin of width $\pm 15\%$ about the center of the peak in M . A bin width of $\pm 10\%$ or $\pm 25\%$ produces the same significance to within a few percent. In this plot, $m_{\tilde{t}_1} - m_{\tilde{\chi}_1^0} \simeq 201$ GeV. When this difference is reduced to ~ 150 GeV, the signal and background spectra peak in the same location, and sensitivity to the signal begins to be lost.

Performing the same mass reconstruction for a series of top-squark masses, we examine quantitatively the functional dependence of Eq. (5) on λ'' . For most of mSUGRA parameter space, $a\Gamma_{\tilde{t}_1}^{R_p} = 0.01$, and $b\Gamma_{\tilde{\chi}_1^+}^{R_p} = 0.5$. The resulting significance (S/\sqrt{B}) as a function of λ'' is shown in Figs. 10 and 11 for each run of the Tevatron. For $\lambda'' < 0.2$, the significance clearly behaves as $(\lambda'')^2$. This behavior has two important consequences. Since little additional optimization can be made with the cuts to reduce the background, more than 32 fb^{-1} of integrated luminosity would be required in order to improve the bound on λ'' by a factor of 2 at run II. Thus, it will be difficult to set better limits than those presented here. On the other hand, the full run II integrated luminosity is not necessary to approach the limits. Second, since the significance is proportional to $(\lambda'')^2/\sqrt{B}$, the calculation is stable against uncertainties in the background estimation, or higher order corrections to the signal. Even a factor of 2 uncertainty in the background would not shift the limits by more than 20%. If $\lambda'' \approx 1$, the loss of signal is important only for the highest masses we probe. This region might be covered by looking for a peak at large E_{Tb} in the many-jet plus b -tag sample, where the chargino has decayed to three jets.

In Fig. 12 we show the reach in λ'' for $165 < m_{\tilde{t}_1} < 550$ GeV for run I and run II of the Tevatron, and with the first 10 fb^{-1} at the LHC. With an integrated luminosity of 2 fb^{-1} at $\sqrt{S} = 2 \text{ TeV}$, discovery at the level of 5σ is possible provided that $\lambda'' > 0.02 - 0.1$ for top squarks with $165 < m_{\tilde{t}_1} < 400$ GeV. Otherwise, a 95% confidence-level exclusion limit can be set for λ'' as a function of the mass out to about 500 GeV. For the lower integrated luminosity and energy of the existing run I data, values of $\lambda'' > 0.04 - 0.3$ can be excluded at the 95% confidence level if $m_{\tilde{t}_1} = 165 - 350$ GeV. With the large increase in cross section at the LHC, both discovery regions and limits may be extended another order of magnitude in λ'' , and to top-squark masses approaching 1 TeV.

There are two reasons our analysis cannot be extended much below $m_{\tilde{t}_1} \simeq 165$ GeV. One is the loss of signal owing to cuts. While the cuts might be relaxed slightly, they are now close to the limit. The other is a loss of confidence in modeling of the background near and below the peak in the $W - j$ mass distribution. Below this peak, mismeasurement problems and detector effects are significant sources of uncertainty. A detailed experimental analysis may be able to overcome this constraint.

The virtue of probing the λ''_{3jk} couplings directly is that they may be bounded independently if no signal is found. The limits on individual couplings are determined by the relative weights of the corresponding parton luminosities. In Figs. 13 and 14, we show the 95% confidence-level limits that may be placed on λ''_{312} , λ''_{313} , and λ''_{323} independently, as a function of top-squark mass at run I and II of the Tevatron. For $m_{\tilde{t}_1} = 255$ GeV, absence of a signal in run I data means that $\lambda''_{312} < 0.08$, and absence in run II data means that $\lambda''_{312} < 0.03$. The bound on λ''_{312} is strongest because its contribution is proportional to the $d \otimes s$ parton luminosity. Even at run I, a significant improvement can be made in the limits on λ''_{312} and λ''_{313} .

Another aspect of Eq. (5) is apparent in the crossing of the limits for a common λ'' and λ''_{312} . The three possible couplings contribute almost equally to the R_p -violating decays of the top squark and chargino. In contrast, the production rate arises mostly from the λ''_{312} term. Hence, there is a net gain in measurable cross section in the R_p -conserving decay channel if only this coupling is large. At run II, a limit of $\lambda''_{312} < 0.2$ can be placed for top-squark masses up to 550 GeV. Even λ''_{323} may be probed directly if $m_{\tilde{t}_1} < 300$ GeV.

C. mSUGRA

A specific set of parameters is used in the prior section to generate the masses of the top squark and its decay products. In this section we undertake a broader examination of the minimal supergravity model (mSUGRA) parameter space, and we present limits as a function of m_0 and $m_{1/2}$ for various choices of A_0 , $\tan\beta$, and the sign of μ . This study

allows us to conclude that for most of mSUGRA parameter space the top-squark discovery potential and bounds depend most strongly on the top-squark mass alone.

In Fig. 15 we show contours in the $m_0 - m_{1/2}$ plane of the minimum λ'' necessary for a 5σ discovery of the top squark given 2 fb^{-1} of integrated luminosity at run II of the Tevatron. Plots are shown for $A_0 = -300$, $\tan \beta = 4$ and $\tan \beta = 30$, and both signs of μ . The regions of experimental and theoretical exclusion are explained above, in conjunction with Fig. 7. At low m_0 the $\tau \nu \tilde{\chi}_1^0$ decay of $\tilde{\chi}_1^+$ saturates its R_p -conserving branching fraction. Naively, this effect would seem to make the electron and muon signal disappear. However, a small fraction of the taus satisfy the electron or muon tagging conditions. The net effect is an increase in the mass reach in the region of small m_0 , most evident in the contour plots for $\tan \beta = 4$.

The discovery contours of Fig. 15 follow closely the top-squark mass contours. This point becomes evident if one compares Fig. 7 and the top-left-hand pane of Fig. 15 for which the same mSUGRA parameters are used. For example, the contour for $m_{\tilde{t}_1} = 450 \text{ GeV}$ in Fig. 7 and that for $\lambda'' = 0.1$ in the top-left-pane of Fig. 15 can be seen to track each other to reasonable accuracy. The same statement is true also for large $\tan \beta$ and both signs of μ : $\lambda'' = 0.1$ corresponds to $m_{\tilde{t}_1} = 450 \text{ GeV}$.

The only region of significant dependence on the mSUGRA parameters, beyond those that set the top-squark mass, is at low $\tan \beta$ and $\mu < 0$. There is a large suppression of the leptonic branching fractions of the chargino when $|\mu| \sim m_{1/2} \sim m_0$. This suppression is due mostly to a destructive interference between the W boson and sneutrino ($\tilde{\nu}$) decay modes in this region [24]. In terms of physical parameters, $m_{\tilde{\nu}}$ is close to $|\mu|$, and the sign of the $W - \tilde{\nu}$ interference term is the same as the sign of μ . Hence only the region of negative μ is affected. However, the cancellation decouples, as expected, as $m_{\tilde{\nu}}$ becomes heavier than m_W . Dependence of the bounds on the trilinear coupling A_0 is negligible except in the region of small $\tan \beta$ and $\mu < 0$ where it serves as a moderator of the cancellation. As A_0 becomes more positive, the cancellation increases.

The results in Fig. 15 demonstrate that the reach in top-squark mass is significantly

larger in single-top-squark production than it is for pair production, where the latter is restricted to the lower left-hand corner of the plot ($m_0 < 300$ GeV, $m_{1/2} < 170$ GeV) [23].

Contours in the $m_0 - m_{1/2}$ plane of the 95% confidence-level limits (1.96σ) are shown in Fig. 16 for the same parameters as in Fig. 15. Except for the same region of suppression at low $\tan\beta$ and $\mu < 0$, limits can be improved with data from run II at the Tevatron by at least an order-of-magnitude for a broad range of $m_0 < 800$ GeV and $m_{1/2} < 300$ GeV. Since limits on λ'' follow contours of constant top-squark mass, limits on individual λ''_{3jk} couplings can be estimated by comparing Figs. 7 and 14.

V. SUMMARY

In this paper, we extend our study of s -channel production of a *single* top squark in hadron collisions through an R_p -violating mechanism [3]. Even if the R_p -violating couplings λ'' are as small as 0.01, two orders of magnitude below the current bounds, the single-top-squark rate exceeds the pair rate for $m_{\tilde{t}_1} > 100$ GeV. This enhancement will allow searches at the Fermilab Tevatron to reach much higher top squark masses than those based on traditional squark pair-production.

Because of the overwhelming jet rate from standard strong interaction processes, R_p -violating production of top squarks followed by R_p -violating decay into a pair of jets is not a viable means to exclude R -parity-violating production of top squarks or to obtain useful bounds on $m_{\tilde{t}_1}$ or λ'' .

We study observability of single top squarks by focusing on the clean R_p -conserving decay, $\tilde{t}_1 \rightarrow b\tilde{\chi}_1^+$, with $\tilde{\chi}_1^+ \rightarrow l^+ + \nu_l + \tilde{\chi}_1^0$. The combined branching fraction for this cascade decay is of order 20% or greater for $\lambda'' < 0.1$, a region of significant interest. We address the case where the neutralino either decays outside of the detector volume or leaves remnants that are too soft to identify; its signature is missing energy in the detector. We simulate both the signal and standard model background processes, including parton showering and hadronization as well as a full detector simulation. We investigate sensitivity to parameters

in our analysis by exploring a wide range of the parameter space of the minimal supergravity model of supersymmetry breaking.

With an integrated luminosity of 2 fb^{-1} at $\sqrt{S} = 2 \text{ TeV}$, we show that discovery of a top squark with $m_{\tilde{t}_1} < 400 \text{ GeV}$ at the level of 5σ is possible provided that the R_p -violating coupling $\lambda'' > 0.02 - 0.1$. Otherwise, a 95% confidence-level exclusion limit can be set for λ'' as a function of the mass out to about 500 GeV. For the lower integrated luminosity and energy of the existing run I data, values of $\lambda'' > 0.05 - 0.2$ can be excluded at the 95% confidence level if $m_{\tilde{t}_1} = 165 - 350 \text{ GeV}$. These limits would constitute a significant improvement over the current 95% confidence-level upper bounds of $\lambda'' \lesssim 1$ for squarks of the third generation. With the large increase in cross section at the CERN Large Hadron Collider, the discovery region and limits may be improved by another order of magnitude in λ'' and extended to top-squark masses approaching 1 TeV. The discovery reach, or exclusion limits, at the Tevatron and LHC depend almost exclusively on the value of the top-squark mass, largely independent of other mSUGRA parameters. Since the R -parity violation occurs only at the production stage, the λ''_{3jk} couplings may be bounded independently if no signal is found. Even at run I, a significant improvement can be made in the limits on λ''_{312} and λ''_{313} .

We propose a simple method to directly probe R -parity-violating couplings at hadron colliders. This analysis searches for a single top squark that is produced in the s -channel via a baryon-number-violating interaction, and decays via standard R -parity-conserving interactions. This strategy should be extended to other squarks and R -parity-violating couplings.

ACKNOWLEDGMENTS

We thank Tom LeCompte and Steve Kuhlmann for valuable advice. We acknowledge communications with Peter Richardson regarding the use of ISAWIG and with Tilman Plehn regarding the use of his NLO K -factors. This work was supported by the U.S. Department

REFERENCES

- [1] P. Fayet, Nucl. Phys. **B90**, 104 (1975); A. Salam and J. Strathdee, Nucl. Phys. **B87**, 85 (1975).
- [2] B. Allanach *et al.*, in *Proceedings of the Workshop on Physics at Run II – Supersymmetry/Higgs*, Fermilab, 1998 (to be published), hep-ph/9906224; G. Bhattacharyya, D. Choudhury, and K. Sridhar, Phys. Lett. B **355**, 193 (1995); O. Lebedev, W. Loinaz, and T. Takeuchi, Phys. Rev. D **62**, 015003 (2000).
- [3] E. L. Berger, B. W. Harris, and Z. Sullivan, Phys. Rev. Lett. **83**, 4472 (1999).
- [4] S. Dimopoulos, R. Esmailzadeh, L. J. Hall, J.-P. Merlo, and G. D. Starkman, Phys. Rev. D **41**, 2099 (1990).
- [5] H. E. Haber and G. Kane, Phys. Rep. **117**, 75 (1985); H.P. Nilles, Phys. Rep. **110**, 1 (1984).
- [6] G. Corcella, I. G. Knowles, G. Marchesini, S. Moretti, K. Odagiri, P. Richardson, M. H. Seymour, and B. R. Webber, hep-ph/0011363.
- [7] J. S. Conway *et al.*, in *Proceedings of the Workshop on Physics at Run II – Supersymmetry/Higgs*, Fermilab, 1998 (to be published), hep-ph/0010338, p. 39.
- [8] A. Chamseddine, R. Arnowitt, and P. Nath, Phys. Rev. Lett. **49**, 970 (1982); R. Barbieri, S. Ferrara, and C. A. Savoy, Phys. Lett. B **119**, 343 (1982); L. J. Hall, J. Lykken, and S. Weinberg, Phys. Rev. D **27**, 2359 (1983).
- [9] S. Weinberg, Phys. Rev. D **26**, 287 (1982); N. Sakai and T. Yanagida, Nucl. Phys. **B197**, 533 (1982).
- [10] P. Slavich, hep-ph/0008270.
- [11] T. Plehn, Phys. Lett. B **488**, 359 (2000).
- [12] W. Beenakker, M. Krämer, T. Plehn, M. Spira, and P. M. Zerwas, Nucl. Phys. **B515**

- 3, (1998).
- [13] H. Murayama, I. Watanabe, and K. Hagiwara, KEK Report 91-11, January 1992.
 - [14] CDF Collaboration, F. Abe *et al.*, Phys. Rev. D **48**, 998 (1993).
 - [15] K. Hikasa and M. Kobayashi, Phys. Rev. D **36**, 724 (1987).
 - [16] S. D. Ellis and D. E. Soper, Phys. Rev. D **48**, 3160 (1993).
 - [17] T. Sjöstrand, P. Eden, C. Friberg, L. Lonnblad, G. Miu, S. Mrenna, and E. Norrbin, hep-ph/0010017.
 - [18] H. Dreiner, P. Richardson, and M. H. Seymour, JHEP 04, 008 (2000).
 - [19] T. Stelzer and W. F. Long, Comput. Phys. Commun. **81**, 357 (1994).
 - [20] H. L. Lai, J. Huston, S. Kuhlmann, J. Morfin, F. Olness, J. F. Owens, J. Pumplin, and W. K. Tung, Eur. Phys. J. **C12**, 375 (2000).
 - [21] F. E. Paige, S. D. Protopopescu, H. Baer, and X. Tata, Brookhaven Report BNL-HET-99-43, hep-ph/0001086.
 - [22] L3 Collaboratuion, *Search for Charginos and Neutralinos in $e+e-$ collisions at $\sqrt{s} = 192-202$ GeV*, L3 Note 2583.
 - [23] V. Barger *et al.*, in *Proceedings of the Workshop on Physics at Run II – Supersymmetry/Higgs*, Fermilab, 1998 (to be published), hep-ph/0003154.
 - [24] For a detailed study of $\mu < 0$ and $\tan \beta = 4$, see A. Bartl, H. Fraas, W. Majerotto, and B. Mösslacher, Z. Phys. C **55**, 257 (1992).

TABLES

TABLE I. Cuts used to simulate the acceptance of the detector for the Tevatron run II and run I (in parentheses if different). At the LHC, $|\eta| < 2.5$ for all objects. The “lepton veto” retains leptons with ($E_{Tl} < 45$ GeV). The “jet veto” removes events with hard jets ($E_{Tj} > 30$ GeV) and improves purity while slightly improving significance.

$ \eta_b < 2$ (1)	$E_{Tb} > 40$ GeV
$ \eta_l < 1.5$ (1.1)	$E_{Tl} > 15$ GeV (20 GeV)
$\cancel{E}_T > 20$ GeV	$E_{Tl} < 45$ GeV
$ \eta_j < 2.5$	$E_{Tj} > 30$ GeV

FIGURES

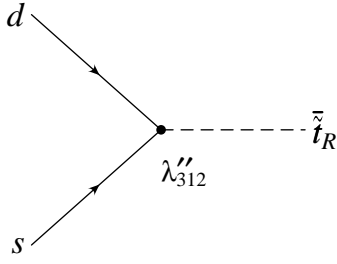


FIG. 1. Feynman diagram for the s -channel production of a single top squark via λ''_{3jk} .

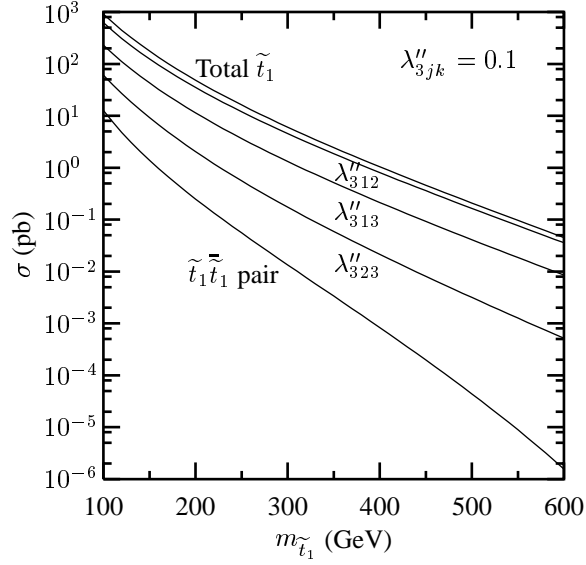


FIG. 2. Cross section versus top-squark mass $m_{\tilde{t}_1}$ for R -parity-violating production of a single top squark at run II of the Fermilab Tevatron ($\sqrt{S} = 2$ TeV) with $\lambda''_{3jk} = 0.1$ compared with the R -parity-conserving production cross section for top-squark pairs.

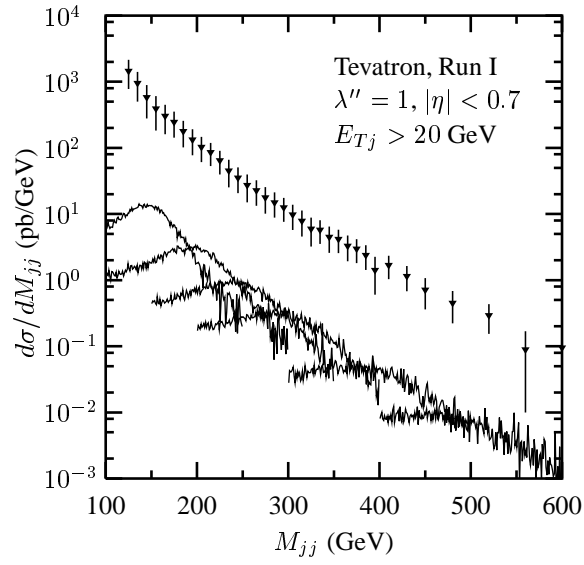


FIG. 3. Dijet mass distribution for the R -parity-violating decay of the top squark at several masses (150, 200, 250, 300, 400, 500 GeV), compared with CDF dijet data from run I of the Tevatron [14].

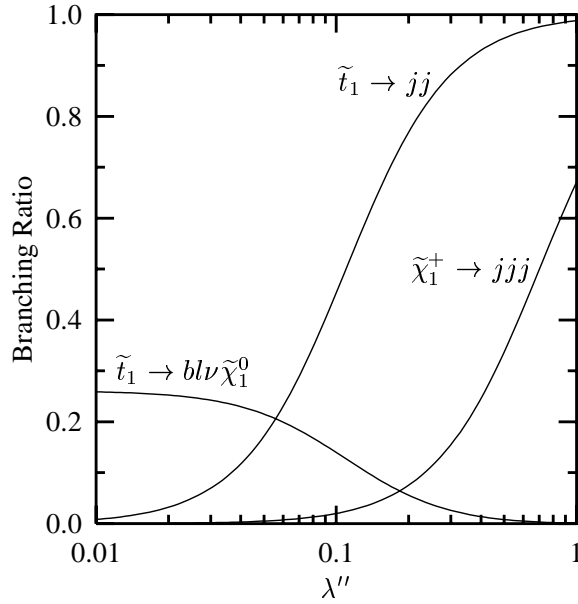


FIG. 4. Branching ratios for the top squark to decay into two jets and for the chargino $\tilde{\chi}_1^+$ to decay into three jets, both as a function of the R -parity-violating coupling λ'' . Also shown is the branching ratio for the top squark to decay into $b l \nu \tilde{\chi}_1^0$.

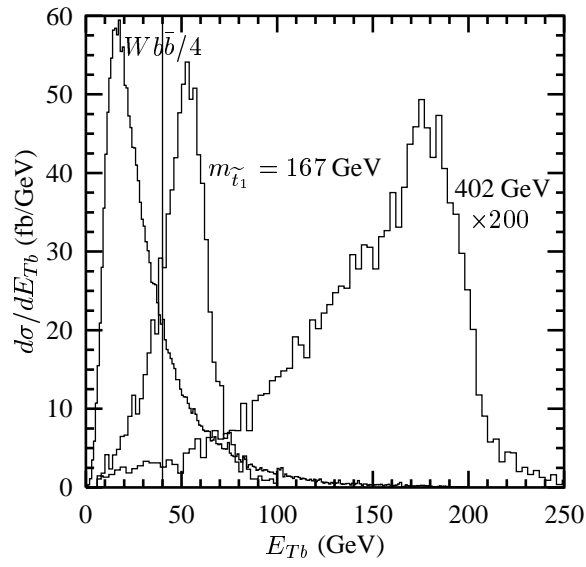


FIG. 5. The transverse energy E_T spectrum (fb/GeV) of the tagged b -jet for top squarks of mass 167 GeV and 402 GeV, and the $Wb\bar{b}$ background at the Tevatron $\sqrt{S} = 2$ TeV. We require $E_{Tb} > 40$ GeV, marked by the vertical line.

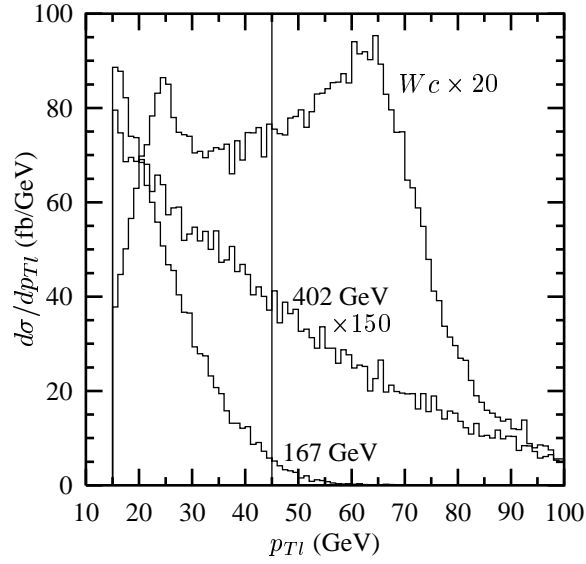


FIG. 6. The transverse momentum p_T spectrum (fb/GeV) of the tagged lepton for top squarks of 167 GeV and 402 GeV, and the Wc background at the Tevatron $\sqrt{S} = 2$ TeV. We require $p_{Tl} < 45$ GeV marked by the vertical line.

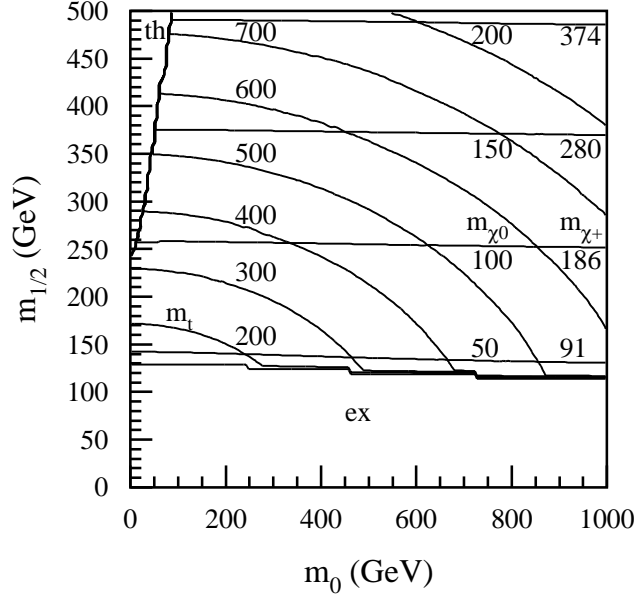


FIG. 7. Contours of constant top-squark mass $m_{\tilde{t}_1}$, chargino mass $m_{\tilde{\chi}_1^+}$ and neutralino mass $m_{\tilde{\chi}_1^0}$ (GeV) through the $m_0 - m_{1/2}$ plane in mSUGRA with $\tan\beta = 4$, $A_0 = -300$, and $\mu > 0$. Theoretically excluded regions are indicated with (th) and experimentally excluded regions with (ex).

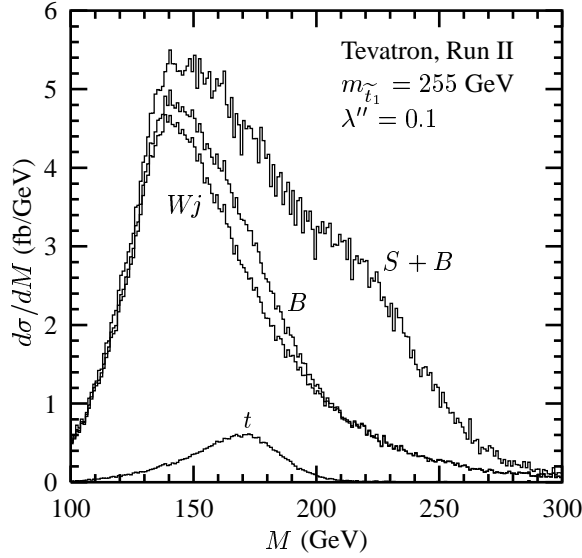


FIG. 8. The reconstructed mass M distribution for single-top-squark production (S) and backgrounds (B) at the Tevatron ($\sqrt{S} = 2$ TeV) for a top-squark mass $m_{\tilde{t}_1} = 255$ GeV and coupling $\lambda'' = 0.1$ with all cuts applied. The Wj component of the background includes Wc , Wj , $Wb\bar{b}$, and $Wc\bar{c}$. The t component of the background includes all single-top-quark production modes ($t\bar{b}j$ is dominant; $t\bar{b}$ and Wt are negligible).

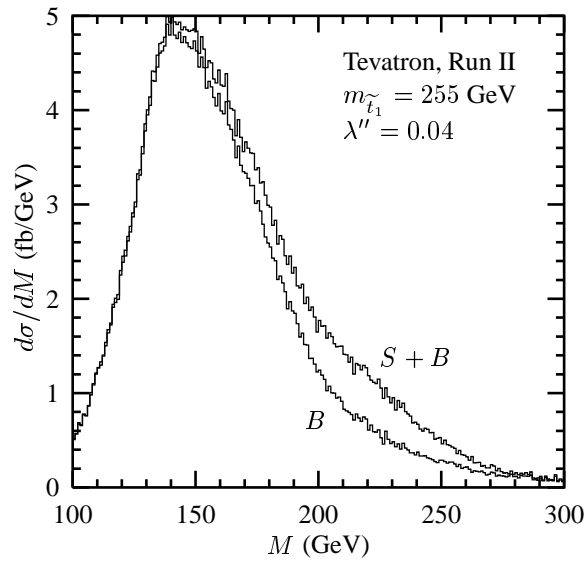


FIG. 9. The reconstructed mass M distribution for single-top-squark production (S) and backgrounds (B) at the Tevatron ($\sqrt{S} = 2$ TeV) for a top-squark mass $m_{\tilde{t}_1} = 255$ GeV with all cuts applied. The coupling $\lambda'' = 0.04$ produces the minimum signal for a 5σ significance at this mass.

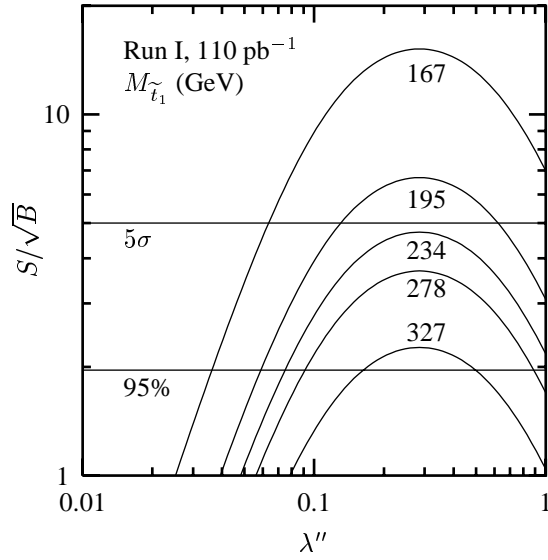


FIG. 10. Statistical significance of the single-top-squark signal (S/\sqrt{B}) in run I of the Tevatron ($\sqrt{S} = 1.8$ TeV, 110 pb^{-1}) versus λ'' for a variety of top-squark masses (GeV).

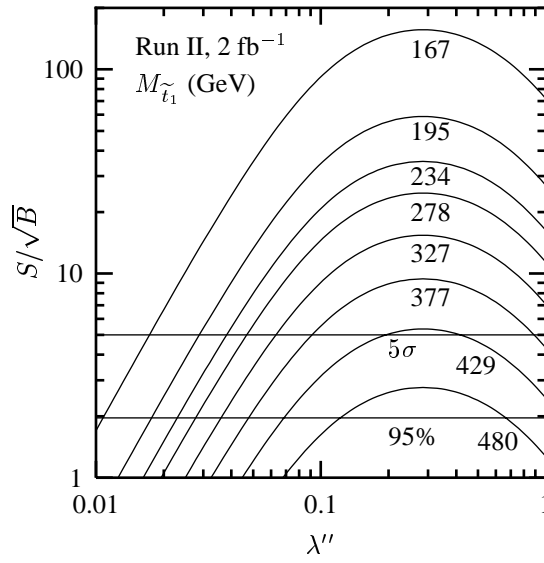


FIG. 11. Statistical significance of the single-top-squark signal (S/\sqrt{B}) in run II of the Tevatron ($\sqrt{S} = 2$ TeV, 2 fb^{-1}) versus λ'' for a variety of top-squark masses (GeV).

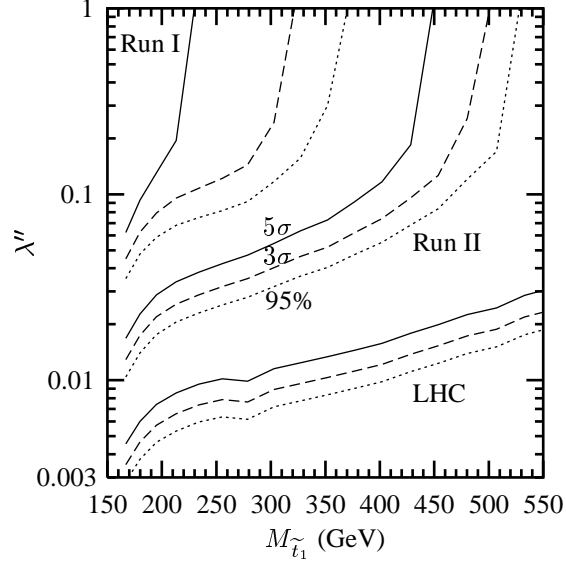


FIG. 12. Lower limits on discovery ($S/\sqrt{B} = 5$, solid), evidence ($S/\sqrt{B} = 3$, dashed), and 95% confidence-level exclusion ($S/\sqrt{B} = 1.96$, dotted) for λ'' versus top-squark mass in run I of the Tevatron ($\sqrt{S} = 1.8$ TeV, 110 pb^{-1}), run II of the Tevatron ($\sqrt{S} = 2$ TeV, 2 fb^{-1}), and one year at the LHC ($\sqrt{S} = 14$ TeV, 10 fb^{-1}).

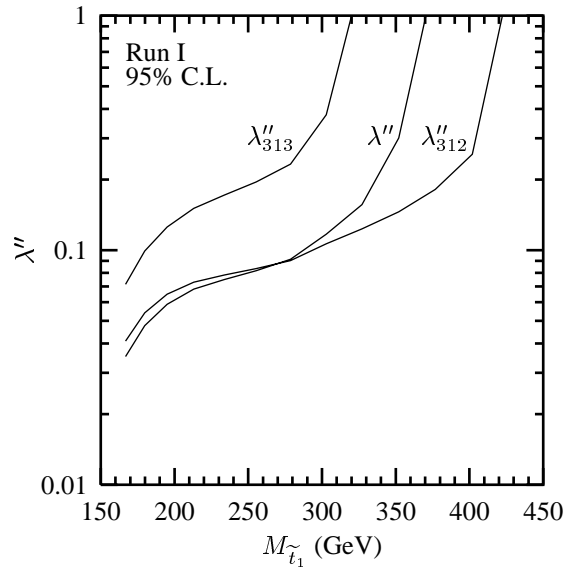


FIG. 13. 95% confidence-level exclusion limits ($S/\sqrt{B} = 1.96$) for λ''_{3jk} versus top-squark mass in run I of the Tevatron ($\sqrt{S} = 1.8$ TeV, 110 pb^{-1}). The curve marked by λ'' is obtained if all three λ''_{3jk} are set equal. There is insufficient rate to obtain a 95% limit on λ''_{323} at run I.

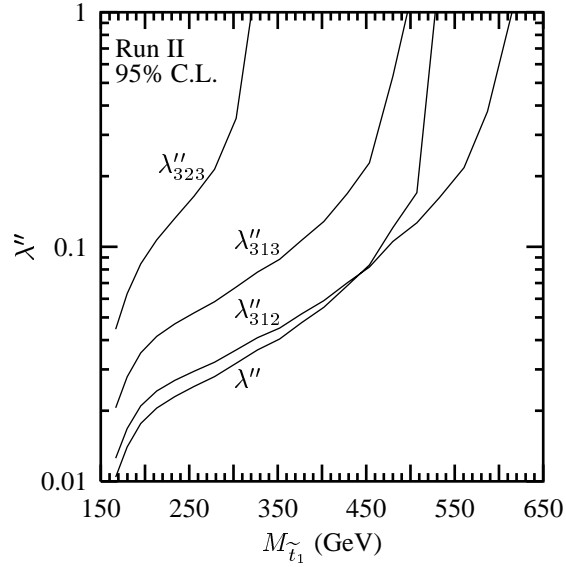


FIG. 14. 95% confidence-level exclusion limits ($S/\sqrt{B} = 1.96$) for λ''_{3jk} versus top-squark mass in run II of the Tevatron ($\sqrt{S} = 2$ TeV, 2 fb^{-1}).

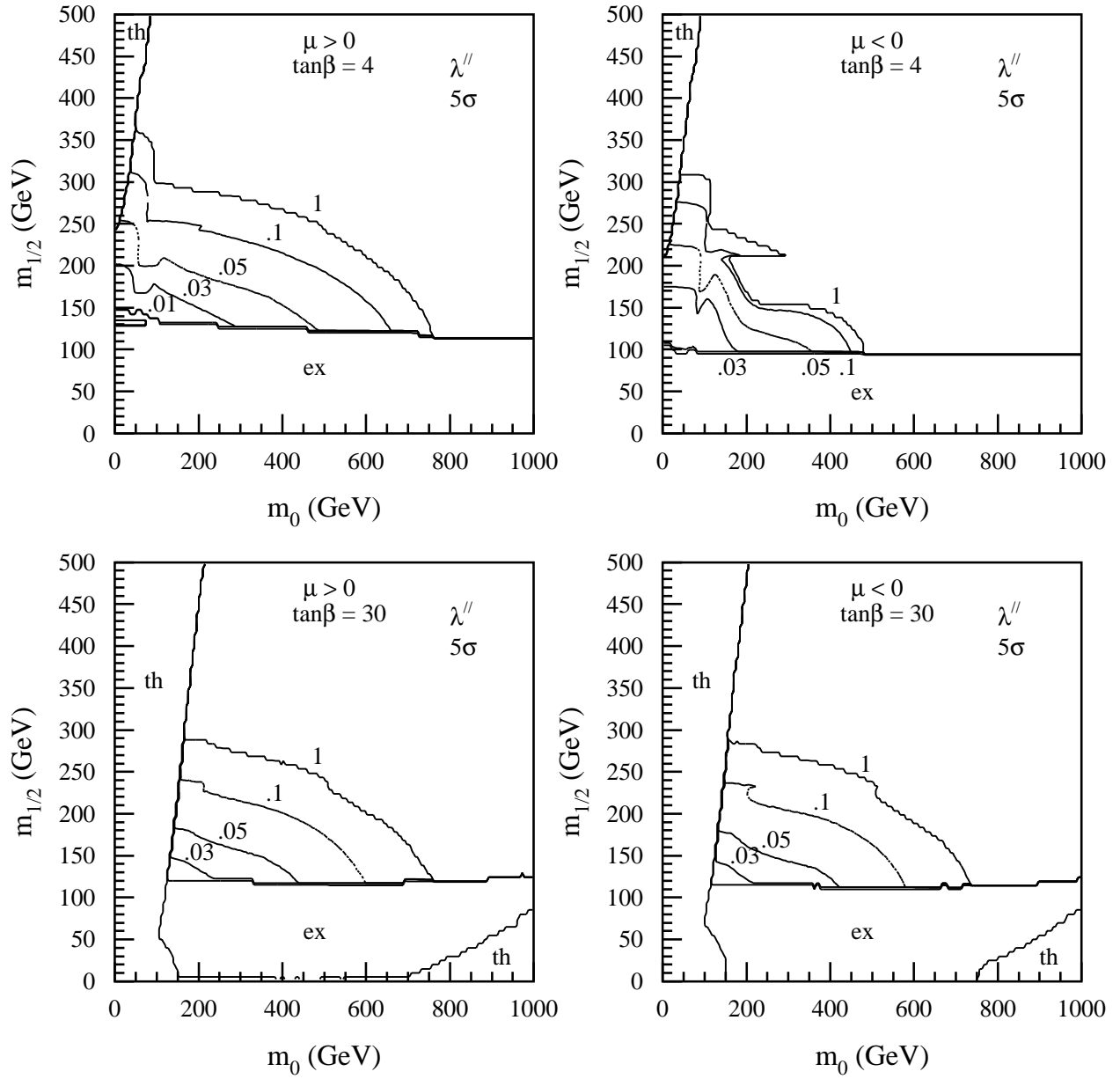


FIG. 15. Contours of the minimum λ'' needed for a (5σ) discovery with 2 fb^{-1} of data at run II of the Tevatron. Four $m_0 - m_{1/2}$ mSUGRA planes are shown with $A_0 = -300$, $\mu > 0$ or $\mu < 0$, and $\tan\beta = 4$ or $\tan\beta = 30$. Theoretically excluded regions are indicated with (th), and experimentally excluded regions are indicated with (ex). For a given λ'' , discovery should occur for values of $m_0 - m_{1/2}$ below and left of the designated contour.

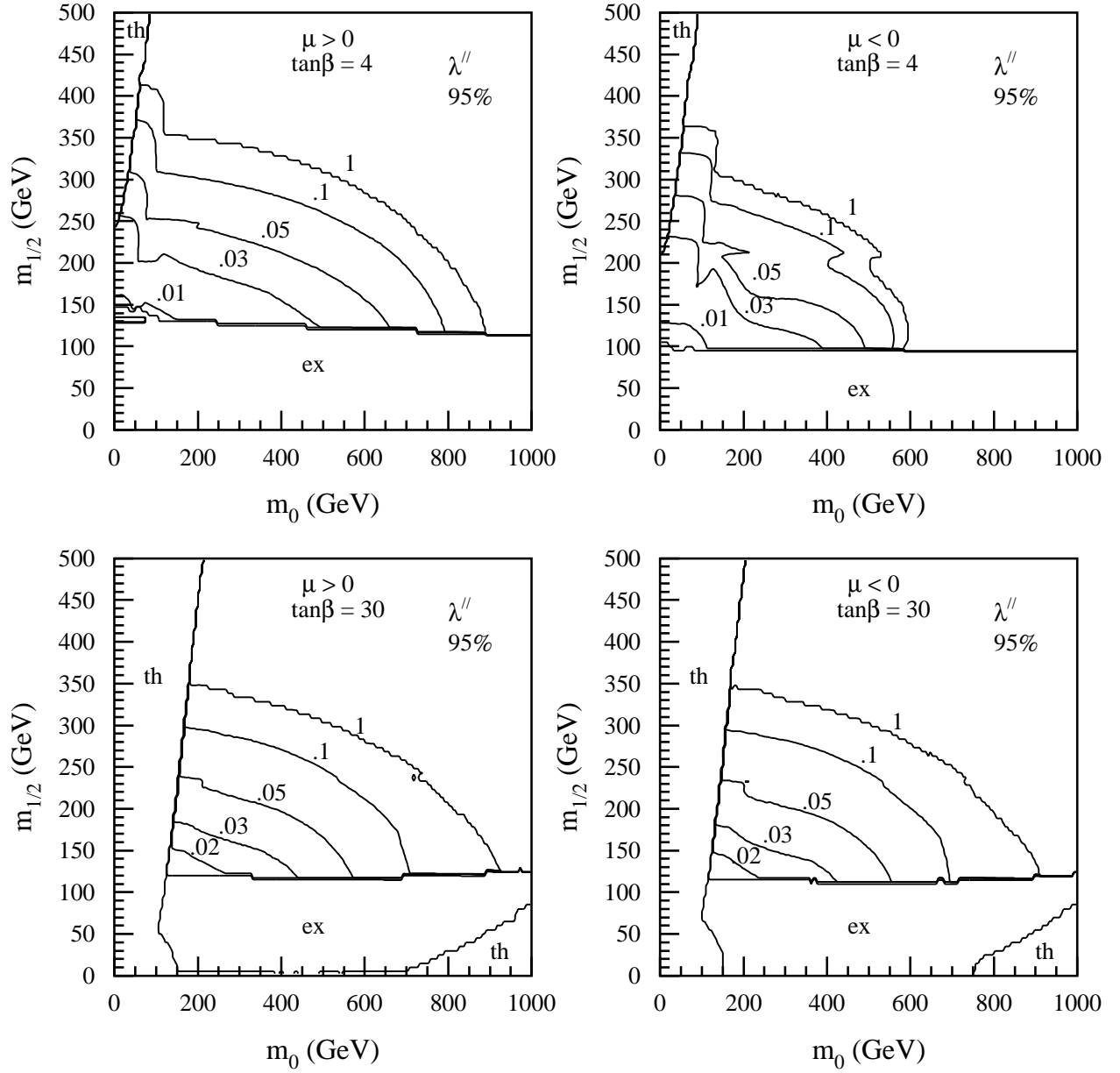


FIG. 16. 95% confidence-level (1.96σ) exclusion contours that can be set for λ'' with 2 fb^{-1} of data at run II of the Tevatron. Four $m_0 - m_{1/2}$ mSUGRA planes are shown with $A_0 = -300$, $\mu > 0$ or $\mu < 0$, and $\tan\beta = 4$ or $\tan\beta = 30$. Theoretically excluded regions are indicated with (th), and experimentally excluded regions are indicated with (ex). Absence of a signal excludes values of λ'' in the region below and left of the designated contour.